Proceedings of the ASME 2021
International Design Engineering Technical Conferences and
Computers and Information in Engineering Conference
IDETC-CIE2021
August 17-20, 2021, Virtual, Online

DETC2021-72123

PRECISE AND EFFECTIVE ROBOTIC TOOL CHANGE STRATEGY USING VISUAL SERVOING WITH RGB-D CAMERA

Danming Wei[1], Christopher M. Trombley, Andriy Sherehiy, Dan O. Popa
Louisville Automation and Robotic Research Institute (LARRI)
University of Louisville, Louisville, Kentucky, USA

ABSTRACT

In modern industrial manufacturing processes, robotic manipulators are routinely used in the assembly, packaging, and material handling operations. During production, changing end-of-arm tooling is frequently necessary for process flexibility and reuse of robotic resources. In conventional operation, a tool changer is sometimes employed to load and unload end-effectors, however, the robot must be manually taught to locate the tool changers by operators via a teach pendant. During tool change teaching, the operator takes considerable effort and time to align the master and tool side of the coupler by adjusting the motion speed of the robotic arm and observing the alignment from different viewpoints. In this paper, a custom robotic system, the NeXus, was programmed to locate and change tools automatically via an RGB-D camera. The NeXus was configured as a multi-robot system for multiple tasks including assembly, bonding, and 3D printing of sensor arrays, solar cells, and microrobot prototypes. Thus, different tools are employed by an industrial robotic arm to position grippers, printers, and other types of end-effectors in the workspace. To improve the precision and cycle-time of the robotic tool change, we mounted an eye-in-hand RGB-D camera and employed visual servoing to automate the tool change process. We then compared the teaching time of the tool location using this system and compared the cycle time with those of 6 human operators in the manual mode. We concluded that the tool location time in automated mode, on average, more than two times lower than the expert human operators.

Keywords: robotic tool change, visual servoing, depth camera, automation.

1. INTRODUCTION

Cameras, as sensors for visual feedback, have routinely been used with robotic manipulators to improve their environmental perception and precision. Vision-based robotic manipulation has been investigated for decades, for operations like grasping [1, 2] and pick-and-place [3, 4]. Traditional cameras only provide image pixel information in color or monochrome mode. But a depth (RGB-D) camera not only can acquire RGB or monochrome images but also can measure the distances between the camera to 3D objects. Thus, based on this advantage of the depth camera, more precise motion and manipulation of robotics have been studied with the RGB-D camera's assistance [5-9]. By implementing cameras as sensors to assist the robotic arms, visual servoing techniques have been proposed to calibrate the motion of the manipulator based on vision feedback in closed-loop control [10-14].

In industrial applications, where robots implement automated operations, the robotic manipulators must be taught to reach desired positions in the workspace by the operators using a teach pendant. Sometimes, in order to complete multiple tasks, a single robotic arm must change different tools for different manufacturing operations. To change different tools, robotic tool changers must be used to complete the tool change process. Most robotic tool changers use pneumatics to lock the master and tool side together. The master side is usually mounted at the end of the robot, whereas the tool side is connected to the tool and placed on the mounting module of the tool change station. Tool change coupler can provide the flexibility to automatically change the end-effectors.

Researchers [15-17] have studies the automatic tool change (ATC) process in robotic systems. For the tool change process, the robotic arm must be taught by the operator to locate the different tools' locations and align the tool change coupler

[1] Danming Wei: danming.wei@louisville.edu

(master side and tool side) properly to lock them together. Then the tools can be removed from the mounting module of the tool change station to accomplish tasks. When the tasks are completed, tools will be placed back in the mounting module. During teaching the tool change process, the operators have to get closed to the tool change station and use their eyes to align the tool change couple properly. But in many non-collaborative robotic systems, it is dangerous to allow the operators inside the system because of the surrounding robotic equipment. A teleoperation tool change process is necessary to avoid the operators exposed to the dangerous robotic environment, however, this is usually a time-consuming process.

In this paper, an RGB-D camera was employed as a sensor to automatically complete the tool change process by using the visual servoing technique. Our custom robotic system, the NeXus was configured as a multi-robot and multi-tool system for multiple tasks including assembly, bonding, and 3D printing of sensor arrays, solar cells, and microrobot prototypes. To assess the cycle-time of a tool change operation, we compared the performance of visual served tool location and exchange, with that of several human operators, including expert users. We found that the automated, camera-based tool change process is more than two times faster than even the expert operators.

The paper is organized in the following orders: in Section 2, we briefly describe the NeXus robotic system and the hardware setup for the tool change process; in Section 3, we detail the methodology used for the automated tool change process; in Section 4, we discuss the results of the completion time in manual mode and automated mode for the tool change process; finally, in Section 5, we conclude the paper and discuss the future work.

2. ROBOT SYSTEM DESCRIPTION

The NeXus is a novel custom robotic system for multiscale additive manufacturing with integrated 3D printing techniques and robotic assembly. The NeXus has several subsystems, such as a microassembly station, an aerosol jetting print station, an intense pulsed light (IPL) photonic sintering station, a fiber weaving station, and a 3D printing station. Material handling and positioning inside NeXus are achieved with the help of a 6-DOF industrial robotic arm and a 4-DOF industrial robotic arm. The 6-DOF ceiling-mounted arm is responsible for substrate and parts tray movement among several additive manufacturing processes. The 4-DOF robot is responsible for pick and place of electronic components for printed circuit board (PCB) applications and positioning tools in conjunction with textile weaving. A tool change station allows two robotic arms to change different tools to complete different tasks. Figure 1 depicts the overall layout of the NeXus.

The NeXus employs a 6-DOF industrial robotic arm, DENSO VS-6577B (DENSO Corporation, CA, USA), which is ceiling mounted on an X-Y gantry (Macron Dynamics, Inc., PA, USA), which is fixed on the top of a custom support frame (Monarch Automation, Inc., OH, USA), and an end-effector with a combination of a depth camera, Intel RealSense d435i (Intel Corporation, CA, USA), ATI Gamma force/torque sensor (ATI Industrial Automation, Inc., NC, USA), and an ATI QC-11 master side is mounted at the end of the robotic arm. ATI QC-11 tool side connected to a HIWIN XEG-32 electrical gripper (HIWIN Corporation, IL, USA) is placed on a tool change station (shown in Figure 2).

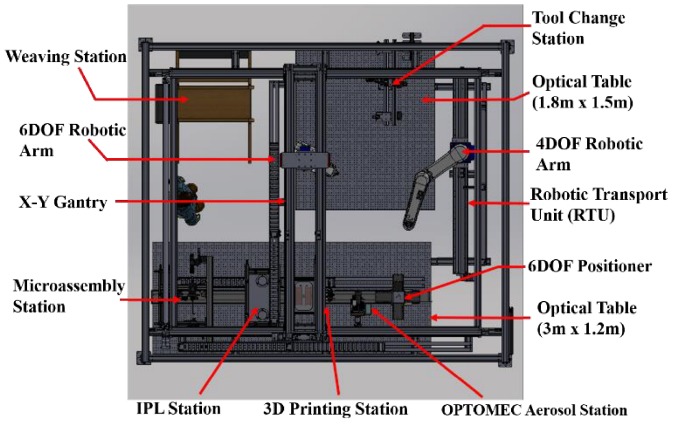

FIGURE 1: TOP VIEW DEPICTION OF THE NEXUS AND ITS SUBSYSTEMS

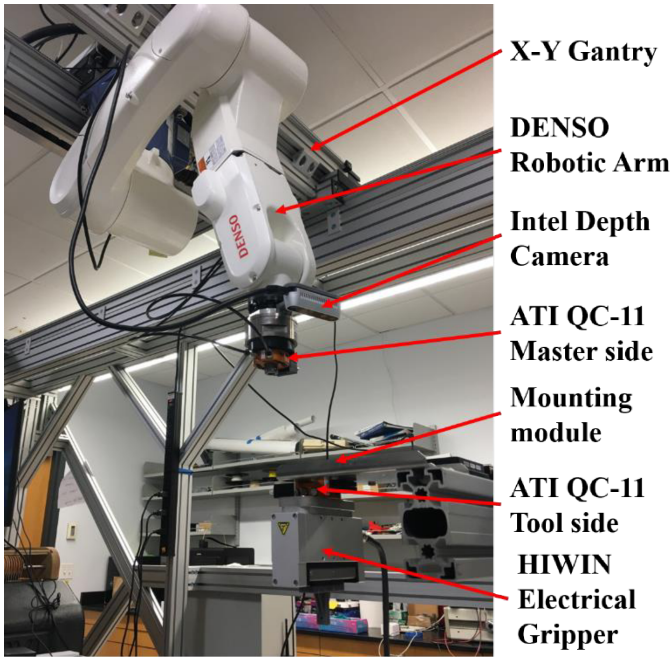

FIGURE 2: HARDWARE SETUP

3. METHODOLOGY

3.1 Tool change process in automated mode

In the automated mode, an initial position was defined to acquire an image of the QC-11 tool side. The distance between the depth camera and surface of the QC-11 tool side was not defined at the beginning of the tool-change sequence. According to the Intel RealSense d435i depth camera's specification, when

the distance between the camera and object is less than 28cm, low-resolution depth values will be acquired. In other words, the distance between the camera and target should not be less than 28cm. Prior to the automated sequence, an image of the QC-11 tool side target was taken at a distance of 30cm from the camera and used as a matching template for the visual servoing process. During the visual servoing process, the origin of the template will be moved to the desired position with the desired orientation. After the visual servoing process, the origin of the QC-11 master side (P_t) will transform to the position of the origin of the camera (P_c) (shown in Figure 3) by homogenous transformation motion. Note that there is no motion in Z-axis during this adjustment. The transformation matrix includes a 2D rotation matrix and a translation matrix employed as equations below:

$$R_z = \begin{bmatrix} \cos\theta & -\sin\theta & 0 \\ \sin\theta & \cos\theta & 0 \\ 0 & 0 & 1 \end{bmatrix} \quad (1)$$

$$T = \begin{bmatrix} 1 & 0 & \Delta x \\ 0 & 1 & \Delta y \\ 0 & 0 & 1 \end{bmatrix} \quad (2)$$

$$P_c = R_z\, T\, P_t \quad (3)$$

$$\begin{bmatrix} X_c \\ Y_c \\ 1 \end{bmatrix} = \begin{bmatrix} \cos\theta & -\sin\theta & 0 \\ \sin\theta & \cos\theta & 0 \\ 0 & 0 & 1 \end{bmatrix} \begin{bmatrix} 1 & 0 & \Delta x \\ 0 & 1 & \Delta y \\ 0 & 0 & 1 \end{bmatrix} \begin{bmatrix} X_t \\ Y_t \\ 1 \end{bmatrix} \quad (4)$$

where R_z is rotation matrix around the Z-axis, T is the translation matrix, θ is the angle between X_c axis and X_t axis. Δx and Δy are the offsets between P_c and P_t in X_c and Y_c axis, respectively, as depicted in Figure 3.

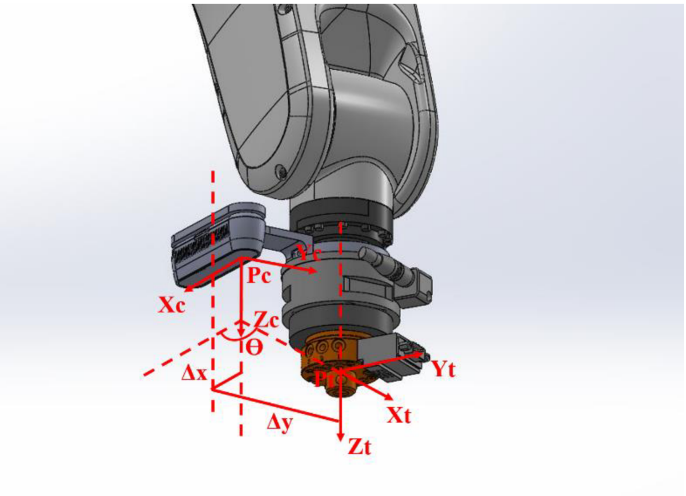

FIGURE 3: COORDINATE SYSTEMS OF CAMERA AND QC-11 MASTER SIDE

After homogenous transformation, the origin of the QC-11 master side was moved to the origin of the depth camera matching its coordinate system. Currently, the QC-11 master side and tool side should be aligned properly with a certain distance. Next step, the robotic arm moved down to make the tool change components coupling, the distance to move down was calculated by measured depth between the camera and surface of QC-11 tool side and the difference between P_c and P_t in Z-axis. Then an internal solenoid valve of the robotic arm was triggered to transfer the compressed air to lock the tool change coupler. According to the QC-11 tool changer mechanism, locking and unlocking the QC-11 master side and tool side can be used pneumatics. After the tool was coupled on the end-effector of the robotic arm, the QC-11 tool side was slid out from the mounting module on the tool change station. The robotic arm moved out in a straight distance and moved back to slide the QC-11 tool side in back to the mounting module. Then, after using compressed air to unlock the tool change components, the robotic arm moved up to release the tool. The whole sequence of the automated tool change process is shown in Figure 4.

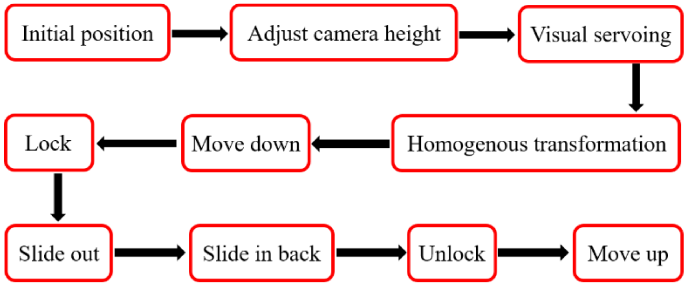

FIGURE 4: TOOL CHANGE SEQUENCE IN AUTOMATED MODE

3.2 Visual servoing

Visual servoing applied into automated mode can enhance the accuracy to locate the position of the QC-11 tool side. With visual feedback, the image Jacobian was employed to adjust the robotic arm motion reaching the desired position and orientation based on the image information of the template. The differences of the origin of template in pixel have the relationship with image Jacobian and differences of robotic arm motions shown in Equation 5. Furthermore, the image Jacobian is a 3x3 matrix expressed in Equation 6 as below [10]:

$$\begin{bmatrix} \Delta P_x \\ \Delta P_y \\ \Delta P_\theta \end{bmatrix} = J_{image} \begin{bmatrix} \Delta X \\ \Delta Y \\ \Delta\theta \end{bmatrix} \quad (5)$$

$$J_{image} = \begin{bmatrix} J_{11} & J_{12} & J_{13} \\ J_{21} & J_{22} & J_{23} \\ J_{31} & J_{32} & J_{33} \end{bmatrix} \quad (6)$$

where ΔX, ΔY, and $\Delta\theta$ are the variations of the robotic motion in a plane; ΔP_x, ΔP_y, and ΔP_θ are variable pixel values of the origin of the template in the field of view of the RGB-D camera. The nine entries of the image Jacobian can be calculated by a set of at least 3 features with known motions of the robotic arm [10,

18]. An image Jacobian generator program was created by LabVIEW® to generate a specific image Jacobian value for a specific magnification of the RGB-D camera with a specific depth between the camera and the surface of the target.

After the image Jacobian was defined, the origin of the template motions to the desired position with the desired orientation can be achieved by the following equation:

$$\begin{bmatrix} X_{new} - X_{cur} \\ Y_{new} - Y_{cur} \\ \theta_{new} - \theta_{cur} \end{bmatrix} = \Delta s \, J_{image}{}^{-1} \begin{bmatrix} P_{X_d} - P_{X_{cur}} \\ P_{Y_d} - P_{Y_{cur}} \\ P_{\theta_d} - P_{\theta_{cur}} \end{bmatrix} \quad (7)$$

where X_{cur}, Y_{cur}, θ_{cur}, X_{new}, Y_{new}, and θ_{new} are the current and new configuration of robotic arm; P_{X_d}, P_{Y_d}, P_{θ_d}, $P_{X_{cur}}$, $P_{Y_{cur}}$, and $P_{\theta_{cur}}$ are pixel values of the desired and current configuration of the origin of the template in the RGB-D camera image. Δs is the step size of the movement of the robotic arm. Based on the vision feedback values, the robotic arm can move to the desired position and orientation in a fast and precise method by using the visual servoing technique.

3.3 Tool change process in manual mode

In the manual mode, we asked six operators with different robotic experiences to complete the tool change process repeatedly 30 times by using the teach pendant. The change completion time was recorded. The operators were requested to start the process at the same initial pose of the robotic arm in the automated mode. Then, they used self-selected speeds and different motions to locate the QC-11 tool side position by the teach pendant. They used their eyes from different viewpoints to align the tool change coupler. After making sure the alignment was properly done, they used the teach pendant to move down to close the QC-11 master and tool sides, then manually controlled the compressed air to lock the tool change coupler. Next, the tool was slid out from the mounting module at a certain distance and slid back to the last location. The tool change coupler was unlocked by controlling the compressed air and then the robotic arm was moved up. The whole sequence of the tool change process in the manual mode is shown in Figure 5.

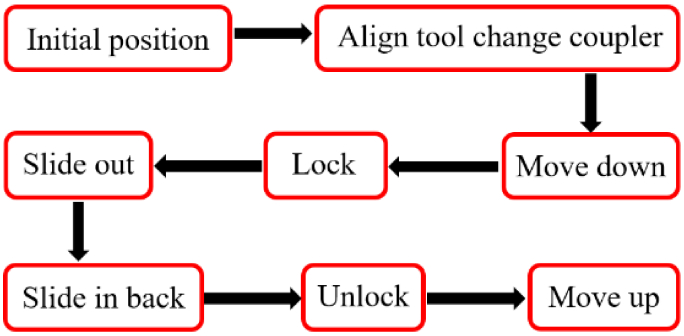

FIGURE 5: TOOL CHANGE SEQUENCE IN MANUAL MODE

4. RESULTS AND DISCUSSION

A LabVIEW® program was created to program the automatic tool change process with a visual servoing function. Figure 6A depicts the image of the QC-11 tool side position from the RGB-D camera at the robotic arm's initial pose. Due to the short distance between the camera and the surface of the tool side, the robotic arm was moving up vertically to reach the 30cm height by coarse and fine movements, and then the visual servoing function was executed to adjust the robotic arm to move target (QC-11 tool side) to the desired position and orientation in the image of the camera. The depth camera had an accuracy of 0.323mm/pixel at the 30cm distance between the camera and the surface of the QC-11 tool side. In Figure 6B, the origin of the target, eventually, was moved to match the center (640, 360) (in pixel) of the image in 1280 x 720 resolution, which was set as the desired position. The orientation was also adjusted to the desired position (0° or 360°).

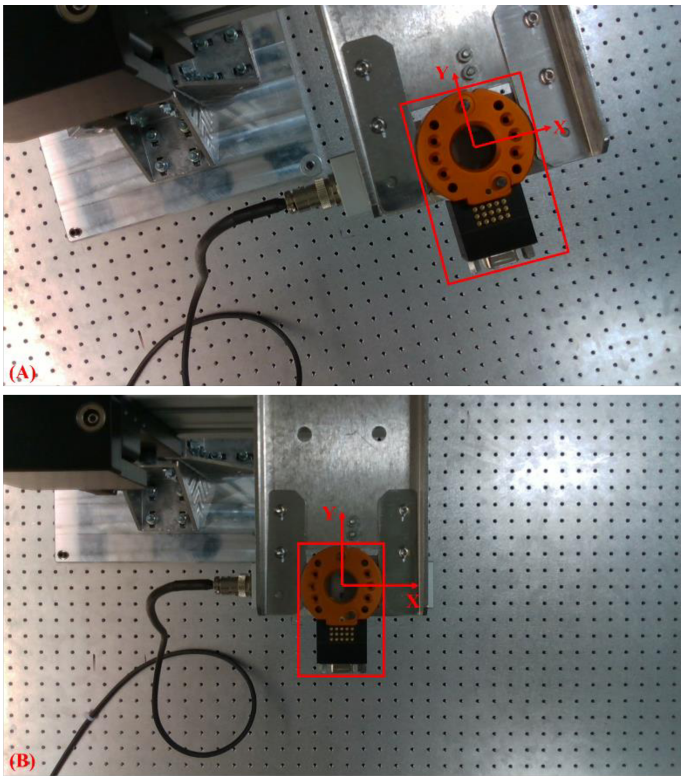

FIGURE 6: (A): IMAGE OF THE QC-11 TOOL SIDE AT THE INITIAL POSITION OF ROBOTIC ARM; (B): IMAGE OF THE QC-11 TOOL SIDE AFTER VISUAL SERVOING PROCESS

While there was +/-1 pixel and +/- 0.1 degrees tolerances in X, Y, and rotation direction respectively configured in the program when the target reached the desired position and orientation. After the visual servoing process, the origin of the QC-11 master side coordinate was transformed to the origin of the camera coordinate. At this moment, the QC-11 master side should be aligned with the QC-11 tool side properly, but there was a constant distance between them. Based on the calibrated

distance from the measured depth value of the RGB-D camera and geometric Z offset between the origin of the camera and the origin of the QC-11 master side, the robotic arm moved down and then locked the tool. After locking the tool, the simple slide-out and slide-in movements were executed in Figure 7. When the tool was back to the mounting module, the tool change coupler would be unlocked, and then move up the robotic arm to apart them.

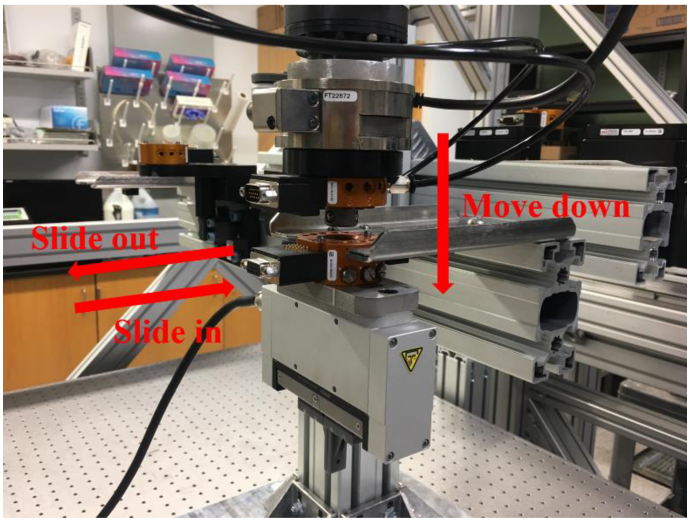

FIGURE 7: MOTIONS OF THE ROBOTIC ARM

In order to evaluate the developed automated control of the 6 DOF robot with the help of the RGB-D camera, we have studied the consistency of the robotic arm task's duration, determined by the time variation from trial to trial. Figure 8a depicts the completion time measurements of the 30 different trials performed in automated mode and for comparison in a manual mode realized by 6 different human operators. It is visible that the time duration of the task in automated mode is significantly shorter with an average time of around 54.2 seconds (Table 1) and a total time of 27 minutes for all 30 trials, whereas for the human operators the best single-trial time was 77s, best average time 103s, and total time around 52 minutes – all for the operator #6, who has much more experience with robotic arm operation. For some other individuals from the testing group, it took significantly longer to finish the task (operator # 5, Table 1) which is related to the level of experience in the operation of the industrial robots or general motorized research tools. On the other hand, even an experienced operator cannot be rush and has to consider the human factor in order to manipulate the robotic arm safely and reliably which can limit further time reduction in completion of the task. Moreover, most of the operators needed the short rests between the trials which were not accounted for in the total time needed to complete 30 trials.

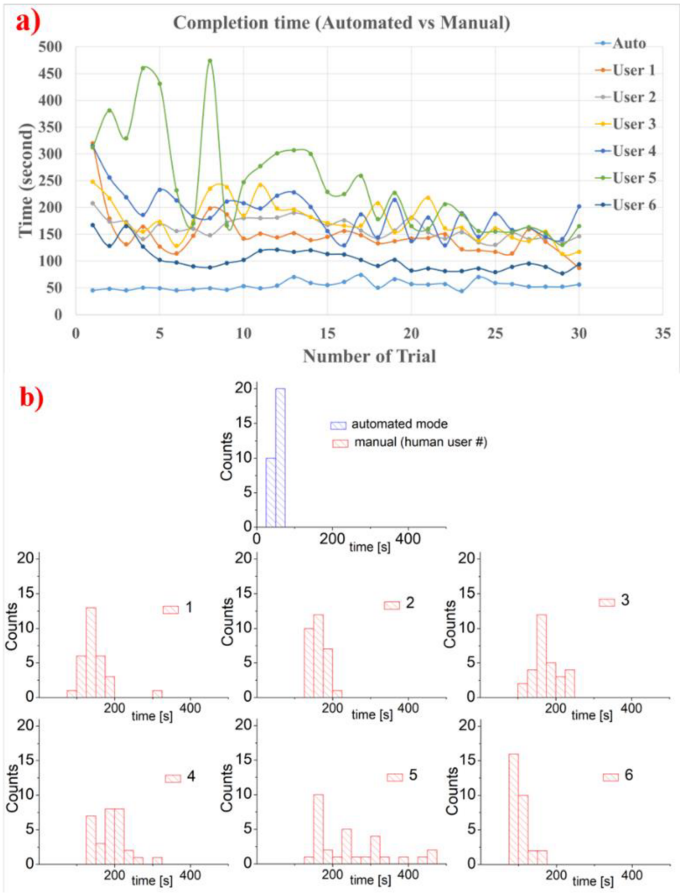

FIGURE 8: (a): COMPARISON OF THE COMPLETION TIME OF THE TOOL CHANGE PROCESS IN AUTOMATED MODE AND MANUAL MODE; (b) DISTRIBUTION OF THE TIME MEASUREMENTS OF THE EXECUTED TASKS FOR THE AUTOMATED (TOP GRAPH) AND MANUAL MODES (SIX GRAPHS AT THE BOTTOM)

TABLE 1: STATISTICAL ANALYSIS OF THE TASK COMPLETION TIME VARIATION OF MANUAL AND AUTOMATED MODES

Mode	Auto	Manual (human operator #)					
		1	2	3	4	5	6
Mean time [s]	54.2	147	161	176	188	243	103
St.Dev. [s]	7.7	39	19	36	41	95	22
Min.time [s]	44	87	130	113	129	130	77
Max.time [s]	74	320	208	248	315	474	167
Total time [min]	27	74	80	88	94	122	52

Another important feature of the presented data is a variation in the time from trial to trial. In the case of the automated mode, results are very consistent (Figure 8a) as indicated by the values of the standard deviation (Table 1). In comparison, for the

manual mode fluctuations of the time between the trials are more significant as it can be clearly seen in Figure 8a, and consequently, values of the standard deviation are much larger compared to the automated mode. For automated mode time values are concentrated in the narrow range between 44 – 74s, in contrast to the manual mode where the time range for all the operators and trials is approximately 77 – 474s.

In a summary, we can conclude that the cycle-time of the automated tool change process is almost more than 2 times faster than expert robot operators. Moreover, the standard deviation is almost 3 times smaller than expert robot operators.

5. CONCLUSION

In this paper, we proposed a visual servoing tool change automated operation for a 6-DOF industrial robotic arm exchanging tools with the NeXus, a custom multi-robot manufacturing cell. An RGB-D camera attached to the robotic arm can improve the precision and reduce the tool pick-up time with the visual servoing technique. Compared with the manual tool pick-up mode by human operators, in the tool change process, the automated mode can reduce completion time by at least 2 times. Especially for inexperienced operators, the automated mode can assist them to complete the tool change process faster and more efficiently. For random tool and multiple tool change processes, the automated mode can enhance the effectivity and precision. Also, avoiding manual teleoperation during the tool change process can prevent human operators from injuries in a non-collaborative robotic environment.

ACKNOWLEDGEMENTS

This work was supported by the National Science Foundation under grant MRI#1828355 and EPSCOR#1849213. We would like to thank the operators who participated in tool-change experiments to collect the completion times of the manual tool change process under IRB.

REFERENCES

[1] Wang, Y., Zuo, B., and Lang, H., "Vision based robotic grasping with a hybrid camera configuration," Proc. 2014 IEEE International Conference on Systems, Man, and Cybernetics (SMC), IEEE, pp. 3178-3183.

[2] Wang, Y., Zhang, G.-l., Lang, H., Zuo, B., and De Silva, C. W., 2014, "A modified image-based visual servo controller with hybrid camera configuration for robust robotic grasping," Robotics and Autonomous Systems, 62(10), pp. 1398-1407.

[3] Luo, G.-Y., Cheng, M.-Y., and Chiang, C.-L., "Vision-based 3-D object pick-and-place tasks of industrial manipulator," Proc. 2017 International Automatic Control Conference (CACS), IEEE, pp. 1-7.

[4] Tsai, C.-Y., Wong, C.-C., Yu, C.-J., Liu, C.-C., and Liu, T.-Y., 2014, "A hybrid switched reactive-based visual servo control of 5-DOF robot manipulators for pick-and-place tasks," IEEE Systems Journal, 9(1), pp. 119-130.

[5] Song, K.-T., Chang, Y.-H., and Chen, J.-H., "3D vision for object grasp and obstacle avoidance of a collaborative robot," Proc. 2019 IEEE/ASME International Conference on Advanced Intelligent Mechatronics (AIM), IEEE, pp. 254-258.

[6] Dzitac, P., and Mazid, A. M., "A depth sensor to control pick-and-place robots for fruit packaging," Proc. 2012 12th International Conference on Control Automation Robotics & Vision (ICARCV), IEEE, pp. 949-954.

[7] Cunha, J., Pedrosa, E., Cruz, C., Neves, A. J., and Lau, N., 2011, "Using a depth camera for indoor robot localization and navigation," DETI/IEETA-University of Aveiro, Portugal, p. 6.

[8] Rennie, C., Shome, R., Bekris, K. E., and De Souza, A. F., 2016, "A dataset for improved rgbd-based object detection and pose estimation for warehouse pick-and-place," IEEE Robotics and Automation Letters, 1(2), pp. 1179-1185.

[9] Mishra, A. K., and Meruvia-Pastor, O., "Robot arm manipulation using depth-sensing cameras and inverse kinematics," Proc. 2014 Oceans-St. John's, IEEE, pp. 1-6.

[10] Wei, D., Hall, M. B., Sherehiy, A., and Popa, D. O., 2020, "Design and Evaluation of Human–Machine Interface for NEXUS: A Custom Microassembly System," Journal of Micro- and Nano-Manufacturing, 8(4), p. 041011.

[11] Hashimoto, K., 1993, Visual servoing, World scientific.

[12] Hutchinson, S., Hager, G. D., and Corke, P. I., 1996, "A tutorial on visual servo control," IEEE transactions on robotics and automation, 12(5), pp. 651-670.

[13] Faria, R. O., Kucharczak, F., Freitas, G. M., Leite, A. C., Lizarralde, F., Galassi, M., and From, P. J., 2015, "A methodology for autonomous robotic manipulation of valves using visual sensing," IFAC-PapersOnLine, 48(6), pp. 221-228.

[14] Wei, D., Hall, M. B., Sherehiy, A., Kumar Das, S., and Popa, D. O., "Design and Evaluation of Human-Machine Interface for NEXUS: A Custom Microassembly System," Proc. ASME 2020 15th International Manufacturing Science and Engineering ConferenceV002T08A018.

[15] Rediger, J., Fitzpatrick, K., McDonald, R., and Uebele, D., 2015, "Fully Automated Robotic Tool Change," No. 0148-7191, SAE Technical Paper.

[16] Gyimothy, D., and Toth, A., "Experimental evaluation of a novel automatic service robot tool changer," Proc. 2011 IEEE/ASME International Conference on Advanced Intelligent Mechatronics (AIM), IEEE, pp. 1046-1051.

[17] Muñoz-Benavent, P., Solanes, J. E., Gracia, L., and Tornero, J., 2019, "Robust auto tool change for industrial robots using visual servoing," International Journal of Systems Science, 50(2), pp. 432-449.

[18] Das, A. N., Zhang, P., Lee, W. H., Popa, D., and Stephanou, H., "μ 3: Multiscale, deterministic micro-nano assembly system for construction of on-wafer microrobots," Proc. Proceedings 2007 IEEE International Conference on Robotics and Automation, IEEE, pp. 461-466.